JOURNAL OF MATERIALS SCIENCE 27 (1992) 3075–3081

Development and properties of a SiC fibre-reinforced magnesium aluminosilicate glass-ceramic matrix composite

B. L. METCALFE, I. W. DONALD, D. J. BRADLEY
Building SB9E3, AWE Aldermaston, Reading, RG7 4PR, UK

The preparation of a magnesium aluminosilicate glass-ceramic matrix composite having an approximately matched thermal expansion coefficient to the silicon carbide fibre reinforcement is described. Data are presented on the process conditions necessary to produce a composite with matched thermal expansion coefficients, the strength and work of fracture of the composite at ambient temperature, and also the effect of temperature on the mechanical properties.

1. Introduction

During the last 25 years much effort has been directed towards producing composites in which the advantages of ceramics, e.g. high intrinsic strength and hardness, high modulus, excellent corrosion and erosion resistance, high-temperature capability, etc. are utilized, but which do not suffer from the disadvantages of ceramics, e.g. low fracture toughness. This has led to the production of ceramic matrix composites with either metal filament or ceramic fibre reinforcement. Early work demonstrated that it was possible to produce tough composites with work of fracture values up to 20 $kJ\,m^{-2}$ for unidirectional ceramic fibre-reinforced [1] and 16 $kJ\,m^{-2}$ for discontinuous randomly orientated metal filament-reinforced composites [2]. It also soon became apparent that because of the large diameter of most of the fibres available, this increase in toughness could only be achieved at the expense of strength due to the concentration of stresses around the fibres. Carbon fibres were one exception to this and various workers achieved simultaneous increases in strength and fracture toughness for composite systems utilizing these fibres [3–7]. Unfortunately, carbon fibres could not be used in oxidizing environments at high ($> 400^\circ C$) temperatures and interest in these systems declined.

During the 1980s, the commercial availability of a wide range of small-diameter ceramic fibres led to a resurgence of interest in ceramic matrix composites [8]. This interest was driven mainly by a desire to increase the operating temperature and therefore efficiency, of jet engines. Composites of silicon carbide fibres in either a glass [9–11] or glass-ceramic matrix [12] have been produced with mean flexural strengths in excess of 1 GPa and work of fracture in excess of 40 $kJ\,m^{-2}$.

Glasses offer advantages over ceramics as a matrix material because they can be processed at much lower temperatures and this minimizes fibre-matrix interaction. Unfortunately, this advantage prevents glass-matrix composites from being used at high temperatures. Glass-ceramics offer a compromise, however, in that they can be consolidated at low temperatures but following crystallization they can be used at higher temperatures than glasses, although not as high as conventional ceramics. An additional advantage of glass-ceramics is that it is possible to modify their thermal expansion coefficients by varying the heat treatment. This, in theory, allows the coefficients of matrix and fibre to be matched, thereby reducing the residual stress in the composite. Work on modifying the thermal expansion of a number of glass-ceramic systems to match the reinforcement has already been reported by the present authors [13, 14]. One system investigated by the authors is a silicon carbide fibre-reinforced magnesium aluminosilicate glass based on the cordierite composition. This was chosen because of the low expansion of cordierite which would assist in matching the expansion coefficients of fibre reinforcement and matrix. Following the presentation of preliminary results on this system [14], further work has now been carried out.

2. Experimental procedure

2.1. Preparation and characterization of the glass-ceramic

A glass (MAS-1, Table I), based close to the cordierite composition but modified by the addition of small amounts of titania and zirconia as nucleating agents and phosphorus pentoxide as a fluxing agent, was prepared as described elsewhere [14]. A modified version of this glass (MAS-2) was made with increased P_2O_5 content as an aid in composite fabrication. Thermal properties of the glasses were characterized by differential thermal analysis (DTA) employing a Stanton Redcroft 673-4 DTA operating at a standard heating rate of $10^\circ C\,min^{-1}$.

0022–2461

TABLE I Composition of glass-ceramics (mol %)

Glass	MgO	Al_2O_3	SiO_2	P_2O_5	TiO_2	ZrO_2
MAS-1	23.4	19.8	48.1	1.4	5.1	2.2
MAS-2	22.5	19.1	46.5	4.9	4.9	2.1

TABLE II. Heat-treatment schedules

Glass-ceramic	Nucleation temperature (°C)	Crystallization temperature (°C)
MAS-2(a)	810	1100
MAS-2(b)	810	1150
MAS-2(c)	860	1100
MAS-2(d)	860	1150
MAS-2(e)	860	1400

The thermal expansion coefficients of glass-ceramic rods were determined using a CDM dilatometer over the temperature range ambient to 700° C for a variety of heat-treatment schedules which are listed in Table II. A minimum of two samples were used in each determination. The bars were held at each temperature for 30 min. Identification of the crystalline phases present was by standard X-ray diffractometry using a Philips PW 1710 diffractometer over the range $2\theta = 10°–80°$.

2.2. Composite fabrication

As-quenched glass frit was ball-milled for 16 h using alumina balls in a porcelain pot.The resulting slurry was then filtered through a 44 μm sieve and dried. Two composite plates, 100 mm × 100 mm × 1.5 mm thick, were manufactured by AEA Technology at Harwell by impregnating a tow of silicon carbide fibres (Tyranno) with the powdered glass dispersed in methyl ethyl ketone and using polyvinyl acetate as the binder. The dried fibre tow was then laid up in a graphite mould and hot-pressed at 810° C for 30 min followed by 1100° C/30 min at a pressure of 13 MPa. Both plates were pressed simultaneously.

2.3. Mechanical testing of composites

The mechanical properties of the composite were determined on bars 50 mm × 5 mm cut from the plate using a diamond cutting wheel. Tests were carried out in three-point bend using a 38 mm span and a crosshead speed of 0.5 mm min^{-1}. From plate 1, 35 specimens were cut and tested at ambient temperature, and 20 specimens cut from plate 2 were tested in batches of five at ambient, 500°, 600° and 700° C, respectively. Elastic modulus was calculated from the load/displacement curves using the crosshead movement as a measure of displacement. Work of fracture values were calculated for some samples by integrating the area under the load/displacement curve; an arbitrary limit of 2.5 times the displacement at peak stress was taken as the limit of useful work of fracture.

2.4. Examination of composites

Fibre distribution within the composite was examined by optical microscopy of polished transverse sections. Fracture surfaces were examined by both optical and scanning electron microscopy.

3. Results and discussion

3.1. Characterization of glass-ceramics

Results of the differential thermal analysis of composition MAS-1 are given in Table III. These showed that this glass had a high glass transition temperature, T_g, and that the high melt start, T_{ms}, and liquidus temperature, T_{liq}, would make composite fabrication difficult. The presence of an exothermic peak, T_{xpl}, proved, however, that it was possible to crystallize this glass. In MAS-2 the increase in phosphorus pentoxide content lowered the melt start by 400° C and the liquidus temperature by 100° C, making fabrication of composites easier and minimizing the risk of reaction between the matrix and fibres.

That the heat treatment can radically alter the thermal expansion coefficient is demonstrated by the results shown in Table IV. These results show that to produce a silicon carbide fibre-reinforced composite with an approximately matched thermal expansion matrix, two possible heat treatments exist (a) and (e). As there is a stronger likelihood of reaction occurring between the matrix and fibres at the higher temperature, leading to either a degradation of the fibres or the production of an undesirable interfacial bond, the plates were crystallized at 1100° C.

X-ray diffractometry of samples with different heat treatments revealed the variation in crystalline phases present and these are listed in Table V.

The XRD analysis of the specimens show some unexpected phases to be present. Three of the heat treatments have led, as expected, to the formation of cordierite, but in each case mullite is present as the major phase. Other workers [15] have noted this in similar cordierite systems and have found it to be very dependent on heat-treatment parameters. Farringtonite (magnesium phosphate) is present in all the low-temperature treatments but no crystalline phase containing phosphorus could be identified in the sample

TABLE III Thermal properties of glasses

Glass	T_g (°C)	T_{xpl} (°C)	T_{ms} (°C)	T_{liq} (°C)
MAS-1	796	1137	1315	1463
MAS-2	763	1097	915	1357

TABLE IV Thermal expansion data

Glass	Thermal expansion coefficient (10^{-6} °C^{-1})	
	20–460°C	(20–700°C)
MAS-2(a)	4.9	4.9
MAS-2(b)	10.0	8.8
MAS-2(c)	8.2	7.6
MAS-2(d)	9.6	8.5
MAS-2(e)	4.7	5.0

TABLE V Variation of crystalline phases with heat treatment

Glass-ceramic	Crystal phases
MAS-2(a)	$MgO{\cdot}Al_2O_3 + ZrTiO_4 + Mg_3(PO_4)_2 + SiO_2$ + glass
MAS-2(b)	$3Al_2O_3{\cdot}2SiO_2 + 2MgO{\cdot}2Al_2O_3{\cdot}5SiO_2$ + $Mg_3(PO_4)_2 + SiO_2$
MAS-2(c)	$MgO{\cdot}Al_2O_3 + 3Al_2O_3{\cdot}2SiO_2 + ZrTiO_4 + SiO_2$
MAS-2(d)	$3Al_2O_3{\cdot}2SiO_2 + 2MgO{\cdot}2Al_2O_3{\cdot}5SiO_2$ + $Mg_3(PO_4)_2 + ZrTiO_4$
MAS-2(e)	$3Al_2O_3{\cdot}2SiO_2 + 2MgO{\cdot}2Al_2O_3{\cdot}5SiO_2 + ZrSiO_4$ + glass

TABLE VI Mechanical properties

Test conditions	Flexural strength (MPa)	Modulus (GPa)	Work of fracture (kJ m^{-2})
Ambient – plate 1	988 ± 76	88.1 ± 6.8	30.2 ± 2.8
Ambient – plate 2	964 ± 73	75.1 ± 2.3	33.6 ± 1.5
500° C	1057 ± 185	92.4 ± 7.4	45.0 ± 4.9
600° C	813 ± 68	87.6 ± 3.4	24.7 ± 3.6
700° C	414 ± 108	78.7 ± 13.8	10.0 ± 48

heated above liquidus temperature. The diffraction pattern of the sample of glass-ceramic treated at 800/1100° C showed that a significant amount of glassy phase still remained indicating that the rate of crystallization is slow at 1100° C. The presence of glass in the sample heated to 1400° C is likely to be due not to a slow rate of crystallization but to the scarcity of nuclei during crystallization. Nuclei and crystals formed during the initial heating stage would redissolve at 1400° C and, on cooling down, the crystallization regime would be encountered before the nucleation regime. In such cases it is probable that surface nucleation due to the large surface area of fibre-matrix interface would predominate. However, in a composite containing 40 vol% fibre, the close proximity of the fibres to each other would generate a matrix with a microcrystalline structure not unlike that produced by heterogeneous nucleation and therefore it should be possible to manufacture composites with a microcrystalline matrix by pressing at this temperature. Carbon was also found to be present in the composites and this results from the incomplete removal of binder before consolidation. XRD of composite surfaces tested at elevated temperatures show a reduction or absence of carbon. This is coupled with a colour change from black to pale grey.

3.2. Mechanical properties

The mechanical properties of the specimens are listed in Table VI. Flexural strengths of four specimens from plate 1 were very much lower than the remaining 31. On examination these specimens were found (a) to have a different failure mode in that an insignificant amount of delamination had occurred, and (b) the fibre distribution in these samples was not uniaxial. For these reasons it was considered permissible to exclude the results of these four specimens from those quoted in Table VI. The mean flexural strengths of specimens tested at ambient and 500° C are very similar, the highest being that of the batch tested at 500° C although this result was distorted by an exceptionally high value (1293 MPa) which also accounts for the large standard deviation associated with this mean.

Specimens tested at elevated temperature were preheated in a muffle furnace prior to testing with the exception of the first one at each temperature which was heated in the test jig. Although this introduced some variability into the time each specimen was at temperature it was considered acceptable, the alternative being a long heating period for each specimen with the consequent slow throughput. This decision was also supported by the work of Mah *et al.* [16] who reported that high-temperature oxygen embrittlement of Nicalon fibres in a lithium aluminosilicate matrix only occurred when the specimen was stressed. No systematic variation was observed in specimens tested at 500° C. At 600° C, however, the first specimen had the highest strength (930 MPa) but the remaining four, although lower, were almost identical (760–798 MPa). At 700° C there was a steady decline in strength between the second and fifth specimens tested.

The observed variation in modulus between the two batches tested at ambient temperature but cut from different plates is probably an artefact resulting from the use of two different test jigs (i.e. different ambient and high-temperature jigs) as the specimen displacement was measured on crosshead movement and not by extensometers on the specimen. Comparison of the results obtained on plate 2 show that there is an increase in modulus up to 500°C followed by a decrease, probably due to the softening of one or more phases present. Although the mean flexural strength of the composite increases only slightly with temperature up to 500°C, the results do show a marked increase (34%) in the work of fracture with temperature. Other authors [9–11, 17–19] have reported flexural strengths which remain constant or increase with increasing temperature up to the glass-transition temperature, whereupon there is a rapid decrease in strength. Such an effect is due to the viscoelastic behaviour of the residual glassy phase within the composite. Brennan and Prewo [11] also reported the variation of K_{IC} with temperature but in none of these references was work of fracture reported.

A stress/strain curve from a specimen tested at 500°C and having a high strength and high work of fracture is shown in Fig. 1. Three regions can be observed within the trace. Up to 375 MPa the trace is a straight line with the composite behaving as a linear elastic solid. Above this stress level progressive multiple matrix cracking occurs causing the trace to deviate from the straight line. The third region shows the failure of the composite as fibres break and the composite undergoes a series of delaminations.

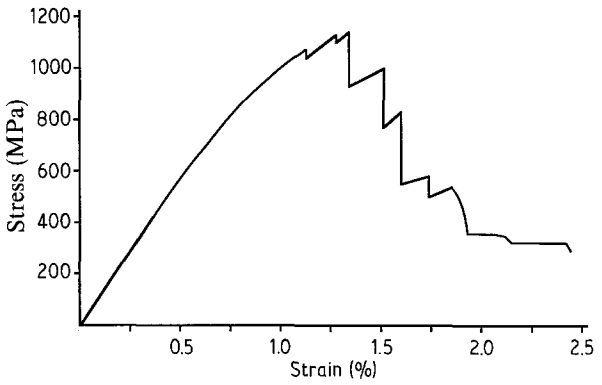

Figure 1 Stress/strain curve of composite tested at 500° C.

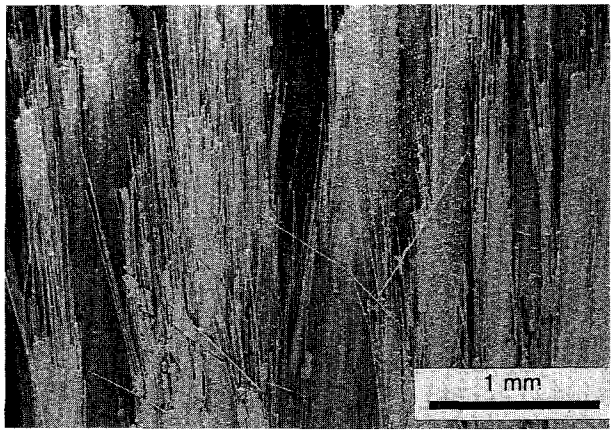

Figure 2 Scanning electron micrograph of fracture surface of the high-strength specimen.

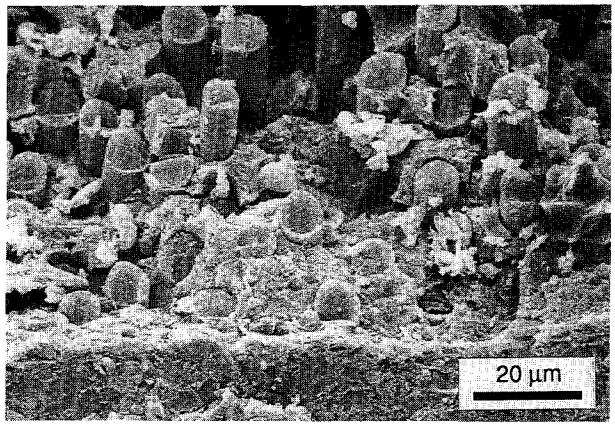

Figure 3 Scanning electron micrograph of fracture surface showing region of brittle failure.

3.3. Microstructure

Scanning electron microscopy (SEM) of the fracture surface of a high-strength specimen tested at ambient temperature (Fig. 2) confirms what would be expected of this specimen. Immediately visible are the fibres which have pulled out of the matrix, in many cases in excess of 1 mm. This behaviour accounts for the high work of fracture. Such behaviour, however, is not uniform across the fracture surface and both brittle failure and delamination are observed. Brittle failure occurs predominately in regions of the composite devoid of fibre reinforcement as is demonstrated in Fig. 3. In the foreground the composite has undergone brittle failure but this has changed to composite failure on entering a region containing fibres, this changeover taking place within a distance of several fibre diameters. Fig. 3 also demonstrates the microcrystallinity of the matrix. This changeover in failure mode from brittle to composite is again demonstrated in Fig. 4 where the brittle failure has led to delamination occurring along a fibre tow. Fig. 5 is unusual in that it shows fibres with a thin surface layer which has become detached in some areas. Such a phenomenon is not visible in the previous micrographs. As the fibres were uncoated before being incorporated into the matrix it must be assumed that this coating is the result of reaction between fibre and matrix. The presence of reaction layers around Nicalon silicon carbide fibres in both lithium aluminosilicate and calcium aluminosilicate matrices has been reported previously [10, 20–23] but these have been either carbon- or silica-rich and much thinner than those currently observed. Also visible are the microcracks in the matrix resulting from exceeding the failure strain of the matrix. The presence of such regions, indicating a high degree of load transfer to the fibres, explains the high strength values obtained with this system. This conclusion is supported by Fig. 6 in which residual

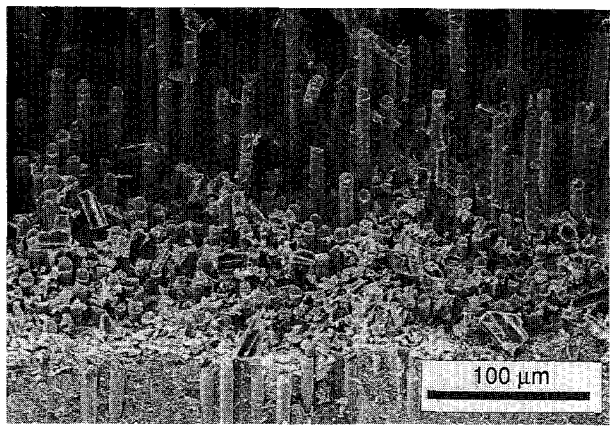

Figure 4 Scanning electron micrograph showing changeover from brittle to composite failure mode.

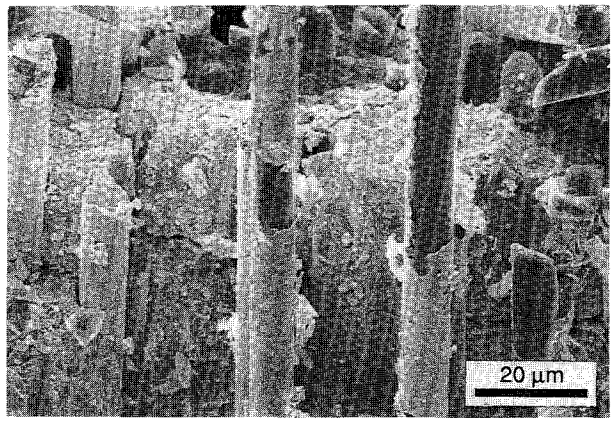

Figure 5 Fibres with a thin reaction layer on their surface.

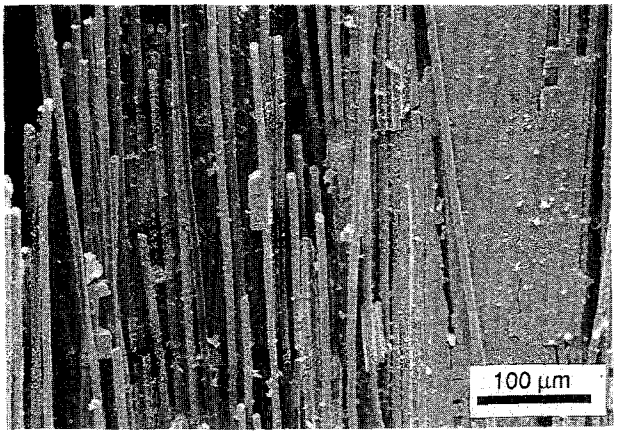

Figure 6 Residual matrix particles still bonded to the Tyranno fibres after testing.

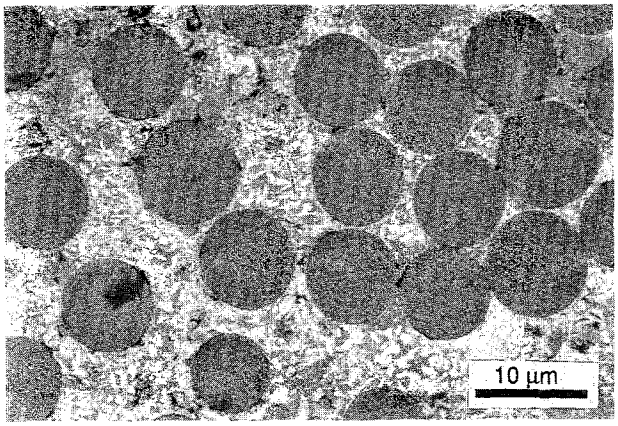

Figure 7 Matrix microstructure as revealed by backscattered electron image of a polished section of composite.

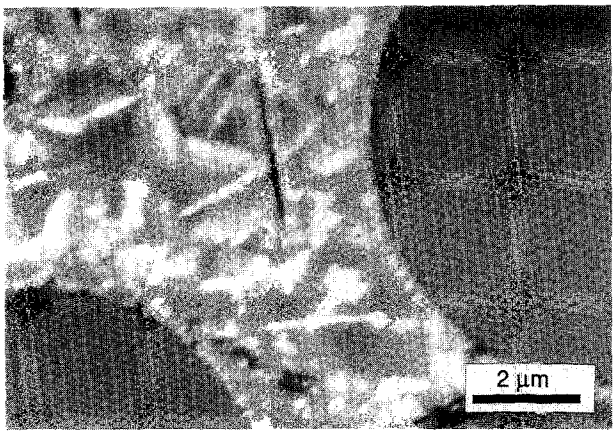

Figure 8 Matrix microstructure as revealed by backscattered electron image of a polished section of composite showing small crystallites nucleated at the fibre surfaces.

matrix particles are shown adhering to fibres. Backscattered electron micrographs of a polished section (Figs 7 and 8) show the matrix microstructure to consist of a mixture of small needle-like grains (< 2 μm long), thin plates and small (< 0.2 μm) particles growing on the other types of crystal and from the surface of the silicon carbide fibres. A low magnification micrograph, Fig. 9, of the tensile surface of one of the specimens excluded from the list of results because of its anomously low strength shows very clearly the non-uniaxial nature of the fibre reinforcement. This is supported by a micrograph of the fracture surface (Fig. 10) which also strongly suggests that the bonding between fibre and matrix is weak as the fibres appear to have very little matrix adhering to them, a conclusion supported by observation of another area of the specimen as shown in Fig. 11. Sbaizero and Evans [24] investigated a symmetric 0°/90° laminated silicon carbide fibre-reinforced lithium aluminosilicate system. They reported a reduction in flexural strength of about 80% when comparing strengths of specimens with one set of fibres parallel to the tensile axis with specimens where both laminates were at 45° to the axis. Although this work

Figure 9 Tensile surface of an anomously low-strength specimen showing poor fibre alignment.

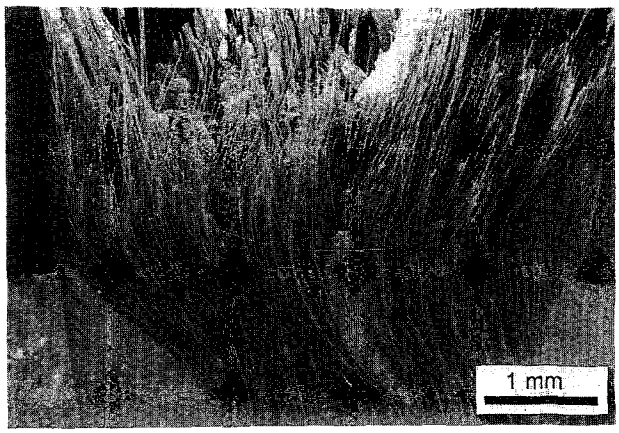

Figure 10 Fracture surface of an anomously low-strength specimen confirming the poor fibre alignment.

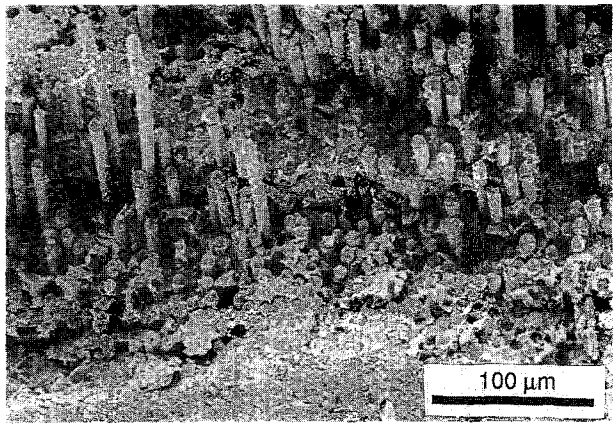

Figure 11 Region of mixed failure modes and poor interfacial bonding.

is not directly comparable with our study, it does demonstrate the serious decrease in strength which occurs when fibres are off-axis. More relevant are the papers by Nardone and Prewo [25] and Hyde [26] in which they show plots of strength versus fibre angle for unidirectional composites. Unfortunately, no details of the composite type are given but again there is a considerable decrease in strength as the off-axis angle increases. Evans and He [27] have demonstrated that fibre debonding occurs more readily in fibres inclined to the stress axis. It is therefore probable that the low strength of this specimen is due to misaligned fibres which result in reduced strength and greater debonding.

Examination of both high- and low-strength specimens tested at 500°C produced very similar micrographs (Figs 12 and 13) to those obtained on the high-strength specimen tested at ambient temperature.That the microstructure of the lowest strength specimen (Fig. 13) should be similar is not surprising because its strength was only slightly lower than the ambient temperature specimen. Regular multiple cracking of the matrix can be observed in this figure.

Like the specimens described previously, those tested at 600°C show both composite and brittle failure regions but the areas of fibre pull-out are decreasing whereas areas of brittle failure are becoming larger (Fig. 14). Also there is a thin surface layer around the composite which has undergone brittle failure. It is not known if this is related to the removal of carbon referred to earlier. The reason for the lower work of fracture is obvious from the reduced amount of fibre pull-out.

Changeover in the failure mode from composite to brittle continues as the temperature is increased and at

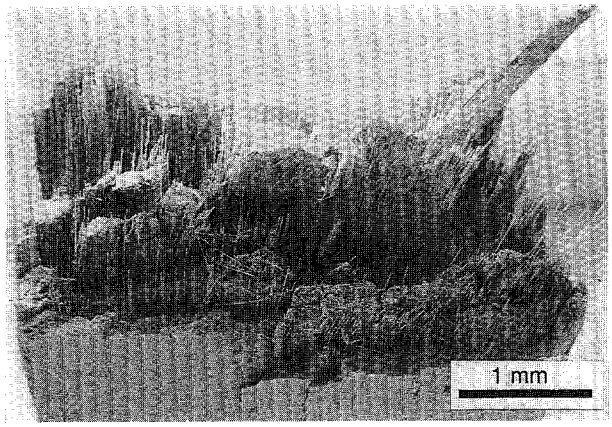

Figure 14 Fracture surface of high-strength composite tested at 600° C.

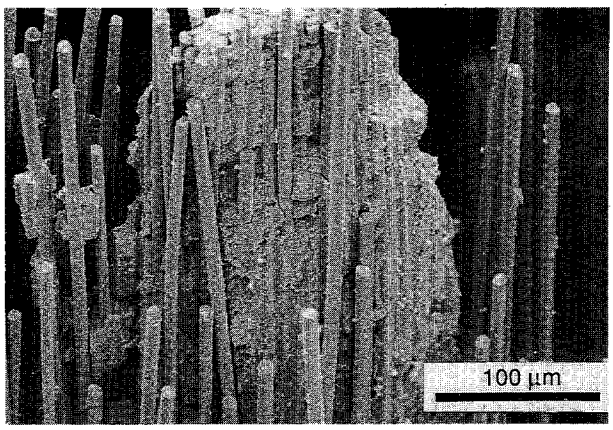

Figure 12 Fracture surface of high-strength composite tested at 500° C.

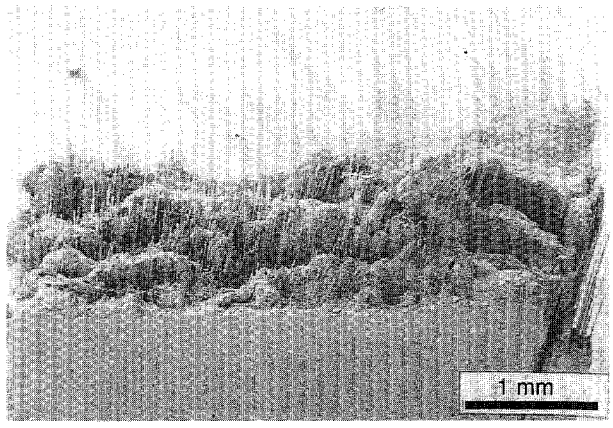

Figure 15 Fracture surface of high-strength composite tested at 700° C.

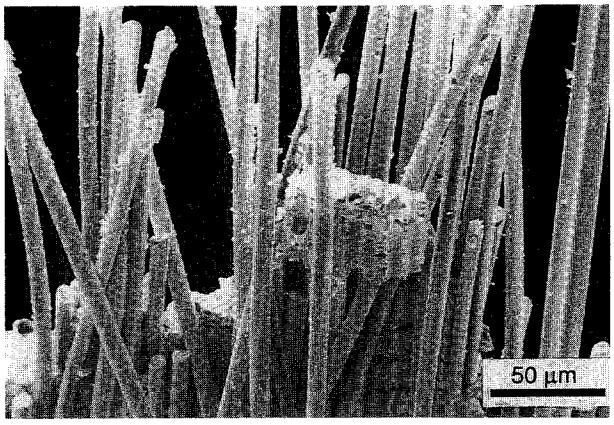

Figure 13 Fracture surface of low-strength composite tested at 500° C.

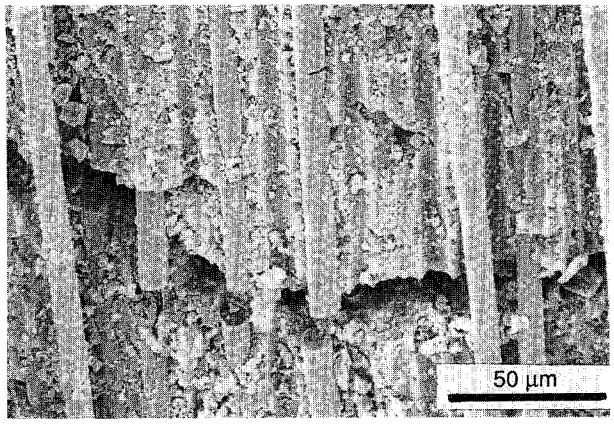

Figure 16 Delamination surface in specimen tested at 700° C.

700°C very little fibre pull-out occurs (Fig. 15). Generally the matrix has fractured into smaller fragments than when tested at lower temperatures. Fig. 16 shows a crack through the matrix normal to a delamination face. This brittle failure mode is very clear, those fibres apparently bridging the crack having become detached at one end.

4. Conclusions

This study has demonstrated that it is possible to manufacture a composite consisting of a magnesium aluminosilcate glass-ceramic matrix reinforced with silicon carbide (Tyranno) fibres. The use of a glass-ceramic for the matrix allows consolidation to be carried out at a much lower temperature (810° C) than is possible for ceramic matrix composites. Conventional fabrication techniques using glass-ceramics usually require consolidation around the liquidus temperature but this study has proved that it is possible to consolidate the composite at a temperature only slightly above the glass transition and simultaneously achieve a low level of porosity. By suitable choice of heat-treatment schedule it is possible to achieve a reasonable thermal expansion match between fibre and matrix, thereby minimizing residual matrix stress caused by differential shrinkage. Mechanical properties of the composite are good with a flexural strength around 1 GPa and a modulus in excess of 75 GPa up to 500°C. Coupled with the high work of fracture, 30 $kJ\,m^{-2}$ at ambient temperature rising to 45 $kJ\,m^{-2}$ at 500°C, this material could fill a gap in the materials field; i.e. a strong, tough material with much better temperature capability than polymeric composites.

Acknowledgements

The authors thank Messrs T. Carter and M. Clay, AWE, for the X-ray diffraction studies and Mr. C. Ruckman, AWE, for the scanning electron micrographs. This paper is published with the permission of the Controller, HMSO, holder of British Crown Copyright 1991/MOD.

References

1. J. A. AVESTON, in 'The Properties of Fibre Composites," NPL Conference Proceedings (IPC Science and Technology Press, Guildford, 1972), pp. 63–74.
2. I. W. DONALD and P. W. McMILLAN, *J. Mater. Sci.* **12** (1977) 290.
3. R. A. J. SAMBELL, A. BRIGGS, D. C. PHILLIPS and D. H. BOWEN, *ibid.* **7** (1972) 663.
4. *Idem, ibid.* **7** (1972)676.
5. D. C. PHILLIPS, R. A. J. SAMBELL and D. H. BOWEN, *ibid.* **7** (1972) 1454.
6. D. C. PHILIPS, *J. Compos. Mater.* **8** (1974) 130.
7. S. R. LEVITT, *J. Mater. Sci.* **8** (1973) 793.
8. I. W. DONALD, *ibid.* **24** (1989) 4177.
9. K. M. PREWO and J. J. BRENNAN, *ibid.* **15** (1980) 463.
10. *Idem, ibid.* **17** (1982) 1201.
11. J. J. BRENNAN and K. M. PREWO, *ibid.* **17** (1982) 2371.
12. D. M. DAWSON, R. F. PRESTON and A. PURSER, *Silicates Ind.* **53** (1988) 129.
13. B. L. METCALFE and I. W. DONALD, *Silicates Ind.* **56** (1991) 99.
14. I. W. DONALD, B. L. METCALFE and D. J. BRADLEY, Institute of Physics Conference Series No. 111, "New Materials and their Applications", University of Warwick, 10–12 April 1990, edited by D. Holland (Institute of Physics, London, 1990) p. 207.
15. M. D. GLENDENNING and W. E. LEE, "Crystallisation of Cordierite with and without SiC fibres", Presented at University of Sheffield Open Day, 10 May 1990.
16. T. MAH, M. G. MENDIRATTA, A. P. KATZ, R. RUH and K. S. MAZDIYASNI, *J. Amer. Ceram. Soc.* **68** (1985) C-248.
17. K. M. PREWO, J. J. BRENNAN and G. K. LEYDEN, *Ceram. Bull.* **65** (1986) 305.
18. K. M. PREWO, *J. Mater. Sci.* **21** (1986) 3590.
19. J. J. BRENNAN and K. M. PREWO, *UK Pat. Appl.* 2075490 (1981).
20. R. F. COOPER and K. CHYUNG, *J. Mater. Sci.* **22** (1987) 3148.
21. J. J. BRENNAN, External Report of United Technologies Research Center No. R84-916018-4 (1984).
22. R. CHAIM and A. H. HUER, *Adv. Ceram. Mater.* **2** (1987) 154.
23. L. A. BONNEY and R. F. COOPER, *J. Amer. Ceram. Soc.* **73** (1990) 2916.
24. O. SBAIZERO and A. G. EVANS, *ibid.* **69** (1986) 481.
25. V. C. NARDONE and K. M. PREWO, *J. Mater. Sci.* **23** (1988) 168.
26. A. R. HYDE, *Mater. Design* **10** (1989) 29.
27. A. G. EVANS and MING Y. HE, *J. Amer. Ceram. Soc.* **72** (1989) 2300.

Received 12 February
and accepted 20 June 1991